Published in final edited form as:
Biochemistry. 2011 June 28; 50(25): 5615–5623. doi:10.1021/bi200348q.

Bacillus subtilis Class Ib Ribonucleotide Reductase Is a Dimanganese(III)-Tyrosyl Radical Enzyme†

Yan Zhang‡ and **JoAnne Stubbe***,‡,§

‡Department of Chemistry, Massachusetts Institute of Technology, Cambridge, Massachusetts 02139, United States

§Department of Biology, Massachusetts Institute of Technology, Cambridge, Massachusetts 02139, United States

Abstract

Bacillus subtilis class Ib ribonucleotide reductase (RNR) catalyzes the conversion of nucleotides to deoxynucleotides, providing the building blocks for DNA replication and repair. It is composed of two proteins: α (NrdE) and β (NrdF). β contains the metallo-cofactor, essential for the initiation of the reduction process. The RNR genes are organized within the *nrdI-nrdE-nrdF-ymaB* operon. Each protein has been cloned, expressed, and purified from *E. coli*. As isolated, recombinant (r) rNrdF contained a diferric-tyrosyl radical ($Fe(III)_2$-Y•) cofactor. Alternatively, this cluster could be self-assembled from apo-rNrdF, Fe(II), and O_2. Apo-rNrdF loaded using 4 $Mn(II)/\beta_2$, O_2 and reduced NrdI (a flavodoxin), can form a dimanganese(III)-Y• ($Mn(III)_2$-Y•) cofactor. In the presence of rNrdE/ATP/CDP, $Mn(III)_2$-Y• and $Fe(III)_2$-Y• rNrdF generate dCDP at 132 and 10 nmol min^{-1} mg^{-1} respectively (both normalized for 1 $Y•/\beta_2$). To determine the endogenous cofactor of NrdF in *B. subtilis*, the entire operon was placed behind a Pspank(hy) promoter and integrated into the *B. subtilis* genome at the *amyE* site. All four genes were induced in cells grown in LB medium, with levels of NrdE and NrdF elevated 35 fold relative to the wild type (wt) strain. NrdE and NrdF co-purified in a 1:1 ratio from this engineered *B. subtilis*. The visible, EPR, and atomic absorption spectra of the purified NrdENrdF complex (eNrdF) exhibited characteristics of a $Mn(III)_2$-Y• center with 2 Mn and 0.5 $Y•/\beta_2$ and activity of 318-363 nmol min^{-1} mg^{-1} (normalized for 1 $Y•/\beta_2$). These data strongly suggest that the *B. subtilis* class Ib RNR is a $Mn(III)_2$-Y• enzyme.

Ribonucleotide reductases (RNRs)1 catalyze the conversion of nucleotides (UDP, ADP, GDP, CDP) to deoxynucleotides, providing the monomeric building blocks required for DNA replication and repair (1). RNRs have been classified on the basis of their metallo-

†This research was supported by National Institute of Health grant GM81393 to J.S.

* To whom correspondence should be addressed. stubbe@mit.edu, Tel: (617)253-1814. Fax: (617) 324-0505.

Supporting Information **Available:** Experimental details and data about cloning, expression and purification of $(His)_6$-rNrdE, rNrdF, rNrdI and rYmaB, characterization of rNrdI, in vitro assembly of active $Fe(III)_2$-Y• and $Mn(III)_2$-Y• of rNrdF, and chromatography elution profiles of *Bs* eNrdF purification are presented in SI. This material is available free of charge via the Internet at http://pubs.acs.org.

1Abbreviations: RNR, ribonucleotide reductase; α_2, ribonucleotide reductase large subunit; β_2, ribonucleotide reductase small subunit; r, recombinant; wt, wild type; e, endogenous; eNrdF, NrdF isolated in a complex with NrdE from *Bs;* Y•, tyrosyl radical; CDP, cytidine 5′-diphosphate; dATP, deoxyadenosine 5′-triphosphate; *Bs, Bacillus subtilis; Ec, Escherichia coli;* $Fe(III)_2$-Y•, diferric-tyrosyl radical; $Mn(III)_2$-Y•, dimanganese-tyrosyl radical; *Ca, Corynebacterium ammoniagenes; Ba, Bacillus anthracis; Mt, Mycobacterium tuberculosis; Sa, Staphylococcus aureus; Sp, Streptococcus pyogenes;* SA, specific activity; NrdIhq, NrdI hydroquinone form; NrdIox, NrdI oxidized form; EPR, electron paramagnetic resonance; FPLC, fast protein liquid chromatography; BSA, bovine serum albumin; SDS-PAGE, sodium dodecyl sulfate polyacrylamide gel electrophoresis; TCA, trichloroacetic acid; Ni-NTA, nickel nitrilotriacetic acid; IPTG, isopropyl-β-D-thio-galactoside; Abs, antibodies; Spect, Spectinomycin; DTT, dithiothreitol; *Ll, Lactococcus lactis;* Amp, Ampicillin; β-ME, β-mercaptoethanol; CV, column volume; PMSF, phenylmethanesulfonyl fluoride.

cofactor, essential for the initiation of nucleotide reduction. The class I RNRs use dinuclear metal clusters and have been further subdivided (Ia, Ib, and Ic) based on their metal composition (Figure 1) (2). This composition has remained an issue due to expression of the RNRs in heterologous bacterial systems and addition of metal to crude cell extracts, prejudicing loading of the apo-protein that is often expressed (2). Our recent studies have suggested that biosynthetic pathways are important for class Ia and Ib cofactor assembly and that often proteins in the pathway are absent or not expressed in recombinant hosts (2, 3). In this paper we report isolation and characterization of the *Bacillus subtilis (Bs)* class Ib RNR from recombinant (r) and endogenous (e) sources and the characterization of their metallo-cofactors.

All class I RNRs contain two proteins, α and β, which in the class Ia prokaryotic systems are homodimers and form active $\alpha_2\beta_2$ complexes. α is the site of nucleotide reduction and allosteric effector binding (dATP, TTP, dGTP, ATP) that controls the specificity of reduction. It is designated NrdA for the class Ia and Ic RNRs and NrdE for the class Ib RNRs. β houses the metal cofactor essential to initiate reduction and is designated NrdB for the class Ia and Ic RNRs and NrdF for the Ib RNRs. All class I β proteins are structurally homologous, and the class Ia and Ib RNRs contain identical metal ligands (compare Figure 1a and 1b) (4, 5).

There are a number of important distinctions between the class Ia and Ib RNRs. One is the presence of the N-terminal ATP cone domain (activity site) that binds ATP/dATP and regulates the rate of nucleotide production in NrdA, which is absent in NrdE. A second is that the class Ib RNR genes, *nrdE* and *nrdF*, are almost always found in an operon with *nrdI* encoding an unusual flavodoxin that plays an essential role in formation of the metal cofactor assembled in NrdF in vivo (6-8).

Finally the most intriguing distinction between the class Ia and Ib βs are the metal composition of the cofactors active in nucleotide reduction. The class Ia RNRs contain only a diferric-tyrosyl radical ($Fe(III)_2$-Y•) cofactor (Figure 1A). It can be formed by self-assembly in vitro from apo-NrdB, Fe(II), and O_2 (9), and is identical to the cofactor isolated from endogenous sources (9, 10). The class Ib NrdFs, however, can form either a $Fe(III)_2$-Y• or a dimanganese(III)-Y• ($Mn(III)_2$-Y•) cofactor in vitro and both are active in nucleotide reduction (7, 11, 12). The NrdF $Fe(III)_2$-Y• cofactor can also be formed by self assembly in vitro, with varying degrees of success, in a fashion similar to the class Ia NrdB (2). However, assembly of the $Mn(III)_2$-Y• in vitro requires in addition to apo-NrdF and O_2, Mn(II) and NrdI with the hydroquinone form of its FMN cofactor ($NrdI_{hq}$) (7). $NrdI_{hq}$ is unable to assist Mn(II) loaded NrdB in assembly of a $Mn(III)_2$-Y• cofactor (7). Finally, recent studies of NrdF isolated from endogenous sources, *Eschericia coli* (*Ec)* and *Corynebacterium ammoniagenes* (*Ca*), have shown that they both possess only a $Mn(III)_2$-Y• cofactor (Figure 1B) (4, 8, 12). The activity of βs with $Fe(III)_2$-Y• and $Mn(III)_2$-Y• cofactors raises several issues. One is whether the active form of the cofactor can be modulated by growth conditions and if so, how metallation (mismetallation) is controlled (2, 3). A second is whether all class Ib RNRs utilize $Mn(III)_2$-Y• cofactors or whether there are yet to be identified conditions, where active iron clusters are generated.

We decided to identify the metallo-cofactor of the class Ib RNR from *Bacillus subtilis (Bs)* for several reasons. First, like *Ec*, *Bs* is a well-studied model organism with accessible genetics and biochemistry. Second, in contrast to *Ec* that contains both a class Ia and Ib RNR where the Ia enzyme is essential for normal aerobic growth, *Bs* contains a single, class Ib, RNR that is essential for normal aerobic growth. Finally, many human pathogens (*Bacillus anthracis (Ba), Mycobacterium tuberculosis (Mt), Staphylococcus aureus (Sa)* and *Streptococcus pyogenes(Sp))* also contain a single, class Ib RNR (13) and thus knowledge

about the *Bs* enzyme, might be informative about the metallo-cofactor in these other organisms.

In order to determine the active form of the class Ib RNR in *Bs*, NrdF was isolated from a strain, in which the operon containing the *nrdI, nrdE, nrdF*, and *ymaB* genes was cloned into pDR111 under a Pspank(hy) promoter and then integrated into the *Bs* genome in the *amyE* site (14). All four proteins were expressed and their concentrations were upregulated. NrdE and NrdF were increased 35 fold relative to the wt strain, facilitating RNR purification. Surprisingly, NrdF co-purified with NrdE in a 1:1 ratio (eNrdF is the complex of NrdEF isolated from *Bs*). UV-vis and electron paramagnetic resonance (EPR) spectra of the purified eNrdF resemble those recently reported for *Ec* $Mn(III)_2$-Y• and *Ca* $Mn(III)_2$-Y• NrdF (4, 7, 8, 12). eNrdF in this complex contained 2 Mn/β_2 and 0.5 $Y•/\beta_2$. The four genes from the operon were also individually cloned, expressed, and purified from *Ec* (recombinant proteins isolated from *Ec* are hence designated by an r before the protein name). $Mn(III)_2$-Y• and $Fe(III)_2$-Y• cofactors in rNrdF were reconstituted in vitro from apo-rNrdF, Mn(II), $NrdI_{hq}$ and O_2 in the former case, and Fe(II) and O_2 in the latter case. The $Mn(III)_2$-Y•-rNrdF has activity about 36% of the endogenous enzyme purified from *Bs* (132 vs 363 nmol min^{-1} mg^{-1}) and is 13 times that of the $Fe(III)_2$-Y•-rNrdF (132 vs 10 nmol min^{-1} mg^{-1}). The results together strongly suggest that $Mn(III)_2$-Y• is the active cofactor in the *Bs* class Ib RNR in vivo and that NrdI plays an essential role in its formation.

Materials and Methods

Cloning, expression, and purification of *Bs* N-terminally $(His)_6$-rNrdE, -rNrdF, -rNrdI, and -rYmaB from *Ec*

Details of the cloning, expression, and purification of rNrdE, rNrdF, rNrdI and rYmaB are described in SI. Briefly, the *Bs* NrdE, NrdF, NrdI and YmaB genes were amplified by PCR using the wt *Bs* JH624 genomic DNA (a generous gift from A. Grossman MIT, Biology Department) as a template. The amplified DNA fragments were then cloned into pET14b (Novagen). In this construct each protein has a $(His)_6$-SSGLVPRGSH tag at its N terminus. The resulting plasmids were sequenced and then transformed into BL21 codon Plus cells (Stratagene). A nickel nitrilotriacetic acid (Ni-NTA) affinity column (Qiagen) was employed to purify each His-tagged protein from cells induced at A_{600nm} of 0.8 with 0.2 mM isopropyl-β-D-thio-galactoside (IPTG). To purify rNrdI to homogeneity, an additional DEAE-Sepharose chromatography step was required and is described in SI. All four proteins were purified to >95% homogeneity. The SA of $(His)_6$-rNrdE was 2 nmol min^{-1} mg^{-1} with a 10-fold excess of $Mn(III)_2$-Y• $(His)_6$-rNrdF (73 nmol min^{-1} mg^{-1}). The SA of $Fe(III)_2$-Y• $(His)_6$-rNrdF as isolated (0.2 $Y•/\beta_2$) was 4.5 nmol min^{-1} mg^{-1}.

Antibodies

Polyclonal rabbit antibodies (Abs) against $(His)_6$-rNrdE, -rNrdF, -rNrdI and -rYmaB were produced by Covance Research Products (Denver, PA).

Metal content

Manganese and iron concentrations were determined using a Perkin Elmer Analyst 600 atomic absorption spectrometer with manganese and iron standards from Fluka. Iron content in heterologously expressed and reconstituted NrdFs was quantitated by the ferrozine method (15).

Protein concentration

Concentrations of purified $(His)_6$-rNrdE, -rNrdF, and -rYmaB were determined by A_{280nm} using ε_{280nm} (79.5, 54.8, and 18.5 mM^{-1} cm^{-1} respectively, and 134.2 mM^{-1} cm^{-1} for eNrdF

calculated using Protparam in ExPASy (16) (http://expasy.org/tools/protparam.html). To determine the $(His)_6$-rNrdI protein concentration, trichloroacetic acid (TCA) was added to a final concentration of 3% (17). The FMN was removed by centrifugation at 20,000 × *g* and the pellet was washed with 3% TCA in buffer. The colorless pellet was isolated by centrifugation and re-dissolved in 500 μL 50 mM Tris-HCl, pH 7.6 with 0.1% SDS. The apo-NrdI concentration was determined by A_{280nm} using ε_{280nm} estimated to be 10 mM^{-1} cm^{-1} (16).

Characterization of $(His)_6$-NrdI

The method for determining ε_{449ox} and ε_{610sq} of FMN bound to NrdI was carried out as previously described (18), and is detailed in SI.

Construction of the *Bs* 1B-UP strain

Two primers 5′-TATACTGCTAGCAGTGTTAGTGATGAGAGATTCA-3′ and 5′-AACCGGGCTAGCTTATTCAAGAATATCAACAACAAAC-3′, each containing an NheI site (underlined), were used to amplify the entire class Ib operon (4.1 kb) using wt *Bs* JH624 genomic DNA as a template. The amplified fragment was cloned into pDR111 (a gift from David Rudner, Harvard Medical School) (14), a plasmid containing *lacI* and *specR* (a gene coding for spectinomycin (Spect) resistance), under a Pspank(hy) promoter that is repressed by LacI. The resulting plasmids were isolated and digested with HindIII (NEB) to select for the correct orientation of the insert and designated pDR111-1B-UP. This plasmid was used to transform *Bs* wt strain JH642 (pheA1 trpC2) (19), and the transformants were selected on LB agar plates containing 100 μg/mL Spect. Transformants were then streaked on starch plates and grown at 37°C for 12 h before staining with iodine to select for starch+ colonies. A starch+ phenotype indicates that homologous recombination has occurred at the *amyE* site and that the *amyE* gene has been disrupted. Disruption of the *amyE* gene removes the ability of *Bs* to break down starch, which can be assayed with iodine as described by Cutting and Vander-horn (20).

Cell growth and protein purification of eNrdF

The *Bs* 1B-UP strain was grown in 5 mL LB medium containing 100 μg/mL Spect overnight at 37°C. The starter culture was diluted in 2 L of the same medium containing 1 mM IPTG in a 6 L baffled flask and grown at 37°C with shaking at 200 rpm. At an A_{600nm} of 0.8, the cells were harvested by centrifugation at 3,000 × *g* for 10 min. The cell paste (2.9 g) was resuspended in 10 mL buffer A (50 mM Tris-HCl, pH 7.6, 5% glycerol) supplemented with 1 tablet of protease inhibitor cocktail (Complete Mini, EDTA free, Roche). Cells were then lysed with a French press at 14,000 psi and the cell debris was removed by centrifugation at 48,000 × *g* for 30 min. $(NH_4)_2SO_4$ (40% saturation 243 g/L) was added gradually over 30 min to the stirring cell lysate. The supernatant was collected after centrifugation at 48,000 × *g* for 30 min. Additional $(NH_4)_2SO_4$ was added to 60% saturation (142 g/L) with stirring over 30 min, followed by centrifugation at 48,000 × g for 30 min. The supernatant was discarded. The pellet was re-dissolved in 10 mL buffer A containing 40% $(NH_4)_2SO_4$ (buffer B). This protein solution was loaded on a Butyl Sepharose column (10 mL, 2.5 cm × 2 cm) and the column was washed with 100 mL buffer B at 2.25 mL/min. The protein was eluted with an 80 × 80 mL linear gradient (buffer B to buffer A, 40%-0% $(NH_4)_2SO_4$), and further eluted with 50 mL buffer A at a flow rate of 3.5 mL/min. Fractions were collected every 3 min and those containing RNR activity were pooled and concentrated using an Amicon Ultra YM30 centrifugal concentrator (Millipore). The solution was diluted with 10 × buffer A, reconcentrated to 1 mL, frozen in liquid N_2 and stored at -80°C.

The protein solution (7.5 mg/mL, 1 mL) was then thawed on ice and chromatographed using a Poros HQ 20 FPLC anion exchange column (Applied Biosystems, 1.6 × 10 cm, 20 mL,

flow rate 2 mL/min). The column was equilibrated with 40 mL buffer A containing 300 mM NaCl. Subsequent to loading, the column was washed with 40 mL buffer A containing 300 mM NaCl and the protein eluted with a 120 mL linear gradient, 300-550 mM NaCl in buffer A, followed by 60 mL of 1.5 M NaCl in buffer A. Fractions (2 mL) were collected. NrdEF-containing fractions were identified by SDS-PAGE and RNR activity assays. Fractions 39-42 were pooled and concentrated to 420 μL as above. This protocol resulted in NrdEF purified to ~80% homogeneity.

Enzyme activity assays

All activity assays for rNrdF or eNrdF contained in a final volume of 220 μL: NrdF [eNrdF (0.2 μM), or rNrdF (1 μM)], 2 -10 μM rNrdE (10 fold excess relative to eNrdF/rNrdF), 0.3 mM dATP (or 1 mM ATP), 20 mM DTT, 10 mM NaF, and 0.5 mM [^{3}H]-CDP (ViTrax, 5,700-21,000 cpm/nmol), in 50 mM Hepes, pH 7.6, at 37°C. Aliquots (52 μL) were removed every 5 min over 15 mins. Each sample was then incubated with 10 U of alkaline phosphatase (Roche, from calf intestine), and the amount of dCDP produced was analyzed by the method of Steeper and Steuart (21).

A typical assay of the fractions from the Butyl Sepharose and Poros HQ 20 columns contained in a final volume of 50 μL: 20 μL protein solution from each fraction, 6 μM rNrdE (SA 2 nmol min^{-1} mg^{-1}), 0.3 mM dATP, 20 mM DTT, 10 mM NaF, and 0.5 mM [^{3}H]-CDP (ViTrax, 5700 cpm/nmol), in 50 mM Hepes, pH 7.6. The reaction mixture was incubated at 37°C for 30 min and the reaction was then stopped by heating at 100°C for 2 min. The workup for dCDP formation is as described above.

EPR spectroscop

EPR spectra of NrdF were acquired on a Bruker EMX X-band spectrometer at 77 K or 4 K using a liquid N_2 finger dewar or an Oxford Instruments liquid helium cryostat, respectively. Acquisition parameters were as described (8). Spin quantitation was performed by double integration of the signal and comparison with a copper standard (22) or an *Ec* NrdB sample with known concentration of Y•. Analysis was carried out using WinEPR software (Bruker).

Western blot analyses of NrdE, NrdF, NrdI and YmaB in *Bs* wt and 1B-UP strains

Bs wt and 1B-UP cells grown in LB medium and LB medium with 1 mM IPTG, respectively, were harvested at A_{600nm} ~0.8, and the cell pellets were resuspended in buffer A (2 mL/g cell paste) supplemented with a protease inhibitor cocktail (Roche). The cells were lysed with the French press and centrifuged at 48,000 × *g* at 4°C for 20 min to remove cell debris. Protein concentration of the supernatant was determined using a Bradford assay and BSA as a standard. The supernatant was diluted with 2 × Laemmli buffer (23) and boiled for 5 min at 100°C. Standard curves were generated using known amounts of purified $(His)_6$ -rNrdE, -rNrdF, -rNrdI and -rYmaB (Fig. S4). All samples were loaded onto either a 10% (for NrdE and NrdF) or a 15% (for NrdI and YmaB) SDS-PAGE gel (Bio-Rad) (23). The gel was run at 200 V for 45 min, and the proteins were transferred to nitrocellulose membranes (Whatman) at 100 V at 4°C for 80 min in 50 mM Tris, 40 mM glycine, 20% (v/v) methanol, 0.03% (w/v) SDS. Primary Abs were added at 1:500 dilution. Stabilized Peroxidase Conjugated Goat Anti-Rabbit (H + L) secondary Ab (Thermo Scientific) was used at 1:5000 dilution. The nitrocellulose membranes were developed using SuperSignal West Femto Maximum Sensitivity Substrate (Thermo scientific). A CCD camera (ChemiDoc XRS Bio-Rad) was used to record the blotting signals. The proteins were quantified by analyses of the signal intensities with Quantity One Software (Bio-Rad).

Results

Bs rNrdF heterologously expressed in *Ec* contains a Fe(III)$_2$-Y• cofactor and is enzymatically active

Bs rNrdE and rNrdF, with a $(His)_6$ tag and 10 amino acid spacer appended to their N termini, were cloned from the *Bs* genomic DNA and expressed in *Ec*. Each protein was purified to >95% homogeneity using a Ni-NTA agarose column (Fig. S1A, B). The UV-vis spectrum of the purified rNrdF (Fig. S1C) exhibited absorbance features at 325 nm, 365 nm and 410 nm, associated with a Fe(III)$_2$-Y• cluster. The EPR spectrum at 77 K (Fig. S1D) was identical to that of the iron-loaded *Ba* rNrdF (24) with additional hyperfine structure that is not observed in spectra reported for the iron loaded, class Ib, rNrdFs from *Ca*, *Mt*, *Ec*, and *Sp* (6, 11, 18, 25). The protein as isolated had 0.2 Y•/β_2. When Fe(II) was added to the crude cell lysate prior to its purification, the Y• content increased to 0.8 Y•/β_2 (Table 1) (18). Incubation of iron-loaded rNrdF with 10 equivalent (equiv) of NrdE, [^{3}H]-CDP as substrate and 1 mM ATP or 0.3 mM dATP as an effector, gave activity of 27 and 19 nmol min^{-1} mg^{-1}, respectively (normalized for 1 Y•/β_2) (Table 1). Thus, a Fe(III)$_2$-Y• active cluster can self-assemble in *Bs* rNrdF, although its activity and that of many other class Ib iron-loaded rNrdFs is low in comparison with class Ia Fe(III)$_2$-Y• NrdBs (*Ec* 6000 nmol min^{-1} mg^{-1}) (2).

Bs rNrdI contains FMN and exhibits similar redox properties to *Ec* NrdI

The $(His)_6$-tagged *Bs nrdI* was cloned, the protein expressed, and purified to 95% homogeneity by Ni-NTA and anion exchange chromatographies as described in SI (Fig. S2A). The ε_{449ox} for NrdI with FMN ($NrdI_{ox}$), which has a λ_{max} at 449 nm, was established to be 9.6 mM^{-1} cm^{-1} by determining the amount of dithionite required to reduce $NrdI_{ox}$ to the $NrdI_{hq}$ (SI and Fig. S2B) and using denatured NrdI to determine the amount of protein. NrdI as isolated contained one FMN/monomer. The ε_{610sq} for $NrdI_{sq}$ (Fig. S2B) was determined to be 3.6 mM^{-1} cm^{-1} as previously described for the *Ec* NrdI (18). The maximal percentage of FMN stabilized in the sq form (32%) (Fig. S2B), is similar to that observed for *Ec* NrdI (30%) (18), and lower than that reported for the *Ba* (60%) and *Bc* NrdIs (100%) (26, 27).

rNrdI is required for active Mn(III)$_2$-Y• cluster formation in vitro from rNrdF

Apo-rNrdF was isolated using 1, 10-phenanthroline in the growth media (18, 28) and purified to homogeneity. The assembly of manganese cofactor was carried out by incubation of Mn(II)-loaded β_2 (25 μM) and $NrdI_{hq}$ (50 μM) followed by addition of 1 mM O_2 (7) and incubation for 3 min at room temperature. Kinetic studies showed that the reaction is complete within this time (data not shown). The mixture was then transferred to an EPR tube and analyzed at 77 K (Fig. S3A, blue) (7). Chelex-100 (Na^+ form) was then added to the sample to remove unreacted Mn(II) and the EPR spectrum was again recorded and the spin quantitated (Fig. S3B). A control in the absence of NrdI showed the spectrum of $Mn(H_2O)_6^{2+}$ (Fig. S3A, red). The amount of Mn in the sample was quantitated by atomic absorption. The Y•/β_2 and Mn/β_2 ratios (0.55 and 1.9, respectively (Table S1)), were both substoichiometric, but the Y•/β_2 is higher than those recently reported for the Mn(III)$_2$-Y• in endogenous NrdFs isolated form *Ec* and *Ca* (4, 7, 8, 12).

Apo-rNrdF was also reconstituted with Fe(II) and O_2 to give the Fe(III)$_2$-Y• with 0.9 Y•/β_2 and 2.6 Fe/β_2 (Table S1). The EPR spectrum for the Fe(III)$_2$-Y• cluster is distinct (Fig. S3C) from the Mn(III)$_2$-Y• cluster, as previously demonstrated with *Ec* NrdF (7).

Enzyme activity assays were performed with the reconstituted Mn- and Fe-rNrdFs. Assays were typically carried out with 1 μM rNrdF, 10 μM $(His)_6$-rNrdE (SA 2 nmol min^{-1}·mg^{-1}),

0.5 mM CDP, 1 mM ATP as effector and 20 mM DTT as reductant (21). The activity of Mn-rNrdF was 132 nmol min^{-1} mg^{-1}, while that of Fe-rNrdF was 10 nmol min^{-1} mg^{-1} (Table S1, normalized for 1Y•/β2). Thus both Fe- and Mn- loaded rNrdFs are active, with the activity of the latter being approximately 13 times the former after normalizing for Y•. These results are similar to those recently reported for *Ec* NrdF (7).

Construction of a *Bs* strain (1B-UP) with the four genes in the class Ib operon overexpressed

To facilitate purification of NrdF from *Bs* in sufficient quantities to characterize its metallo-cofactor, a strain was constructed, in which the entire class Ib operon (4.1 kb) was cloned under the Pspank(hy) promoter in pDR111 and integrated into the *amyE* site of the *Bs* JH624 strain (see methods) to give *Bs* 1B-UP (14, 19). The entire operon was cloned in an effort to maintain the relative expression levels of each gene in the operon that could be crucial for metallo-cofactor assembly. Activity assays and Abs raised to rNrdE, rNrdF, rNrdI and rYmaB were used to evaluate the success of our strategy.

The activity of NrdF in crude cell lysates of the wt and 1B–UP strain was determined by addition of excess $(His)_6$-rNrdE. The value of 0.05 nmol min^{-1} mg^{-1} for wt *Bs* is 1600-fold higher than previously reported (29) and that for 1B-UP of 0.9 nmol min^{-1}·mg^{-1} is 18 times that of the wt strain. Western blots of crude cell extracts in both strains revealed that all four proteins were clearly elevated in the 1B-UP strain relative to the wt strain (Figure 2, compare lanes 2 and 3). Quantitative western blots were also performed (Fig. S4) using the recombinant protein standards and the molar ratios of NrdE: NrdF: NrdI: YmaB in the 1B-UP strain were 64: 64: 8: 1. The ratio of NrdE and NrdF relative to the wt strain was increased 35 fold. YmaB was elevated ~10 fold, while NrdI increased 80-190 fold relative to the wt strain. The atypical ribosome binding site of NrdI is likely responsible for its inefficient translation in the wt strain (30). The Pspank(hy) promoter in the 1B-UP strain has resulted in increased transcription as well as more efficient translation.

Purification of eNrdF from the 1B-UP strain

The purification of eNrdF from the 1B-UP strain is summarized in Table 2 and Figure 3. Western blotting revealed that both NrdF and NrdE precipitated between 40-60% $(NH_4)_2SO_4$, and were separated from YmaB and NrdI, which predominantly precipitated with 40% $(NH_4)_2SO_4$ (data not shown). The resulting pellet was redissolved in 40% $(NH_4)_2SO_4$ solution and purified using Butyl Sepharose chromatography (Fig. S5A). Fractions containing RNR activity were pooled, desalted, and then purified further using Poros HQ20 FPLC anion exchange chromatography. The elution profile is shown in Fig. S5B. The appropriate fractions were pooled and stored ~1 mg/mL at -80°C.

SDS-PAGE analysis of each step in the purification is shown in Figure 3A and revealed a band at 75 kDa that co-purified with NrdF. As our $(His)_6$-rNrdE migrated at 75 kDa (80 kDa actual molecular weight), we wondered if the proteins migrating in this region could contain NrdE. Abs to NrdE and western analysis revealed its presence. The ratio of NrdE to NrdF was determined in crude cell extracts by quantitative western analysis and on purified protein (lane 5, Figure 3A) by Coomassie staining in comparison with known concentrations of $(His)_6$-rNrdE and $(His)_6$-rNrdF. In both cases the ratio was 1:1 and the purified eNrdF was judged to be about 80% pure (lane 5, Figure 3A). The co-purification of NrdE and NrdF was unexpected and exciting as in general, the subunit interactions of class I RNRs are weak and the subunits separate during chromatography (31, 32). A unique opportunity for structural characterization crystallographically and by cryoEM thus presents itself.

eNrdF from the 1B-UP strain contains a $Mn(III)_2$-Y• cofactor

A UV-vis spectrum of purified eNrdF is shown in Figure 3B and inset. The spectrum is similar to that of the manganese-reconstituted rNrdF with a sharp peak and broad shoulder at 410 nm and 390 nm, indicative of Y•. The light scattering obscures the broad features observed with the *Ec* $Mn(III)_2$-Y• cofactor from 500 to 600 nm, indicative of oxidized dimanganese clusters (2). The 325 and 365 nm features associated with the diferric cluster (Fig. S1C) are absent (7). eNrdF was also analyzed by EPR spectroscopy at 77K and 4K (Figure 4A and B) and spin quantitation revealed 0.4-0.5 Y•/β_2 (4 independent experiments). These spectra are very similar to our reconstituted $Mn(III)_2$-Y• -rNrdF and to those reported from *Ec* and *Ca* NrdFs (4, 7, 8, 12). Atomic absorption studies revealed that NrdF contained 1.8-2.4 Mn/β_2 and 0.14 Fe/β_2 (Table 3). Thus in all cases of $Mn(III)_2$-Y• detected, metal loading and Y• are substoichiometric.

Activity of $Mn(III)_2$-Y• rNrdF compared with $Fe(III)_2$-Y• rNrdF

The assay for the class Ib NrdF was based on extensive studies of class Ia RNRs. For the Ia RNRs, the α and β subunits separate during purification due to their weak interactions (32) and as a consequence, each subunit is assayed in the presence of an excess of the second subunit to ensure 100% “active” complex formation. In addition, the oxidation of two cysteines in the active site of α to a disulfide accompanies substrate reduction (1), and thus a mechanism for disulfide reduction is essential to measure multiple turnovers of NDP to dNDP. Since the reductant in vivo for most class Ib RNRs has not been extensively studied, the non-physiological reductant dithiothreitol (DTT) is typically used (33). The activity with DTT relative to the endogenous reductant is unknown. Finally, the allosteric regulation of the class Ib enzymes is not as well studied as the Ia enzymes and remains to be examined in a case by case study with the physiologically relevant metallocofactor.

In the assays for the Fe and Mn loaded rNrdF, a 10 fold excess of rNrdE was used, CDP was the substrate, ATP or dATP were the effectors and DTT was the reductant. The ratio of Mn:Fe loaded rNrdF activity, when normalized for 1 Y•/β2, is 132:10. We note that both rNrdE and rNrdF are N-terminally tagged. Removal of the tag from rNrdE and rNrdF, leaving three amino acids (GSH), however, had little effect on activity.

In the assays for eNrdF activity, there is the added complexity that NrdE and NrdF copurify and thus initially no NrdE was added to the assay mixtures. The activity was, however, only 32 nmol min^{-1} mg^{-1} (normalized for 1 Y•/β_2). Thus eNrdF was also titrated with variable amounts of rNrdE (Table S2). With a 10 fold excess, the SA ranged from 318 (Table S2) to 363 nmol min^{-1} mg^{-1} (Table 1, both normalized for 1 Y•/β_2). This number is 3 times higher than the rNrdF (132 nmol min^{-1} mg^{-1}, Table S1) and is 10 and 1000 fold lower than the activity reported recently for $Mn(III)_2$-Y•-NrdF isolated from endogenous *Ec* and *Ca* respectively (4, 8, 12).

The basis for the requirement for excess rNrdE to optimize the activity eNrdF is not understood. The most reasonable explanation is that DTT was excluded from buffers during the purification of eNrdF to prevent reduction of the Y• in NrdF (34). NrdE, is susceptible to oxidation (5 essential cysteines) (35) and thus the low activity may be associated with irreversible oxidation of NrdE in the eNrdF. As noted above, the physiological reductant for the *Bs* RNR would likely increase activity. Finally, rYmaB, the protein in the RNR operon of unknown function (30), has no effect on the catalytic activity.

Although the *Bs* class Ib activity assay requires further optimization, several conclusions are apparent. First, that CDP is more rapidly reduced with ATP than with dATP as the allosteric effector (Table S2, Table 1). These results are distinct from those reported previously for the $Fe(III)_2$-Y• class Ib RNRs (36, 37). The second and major result is that the $Fe(III)_2$-Y•-

rNrdF generated in vitro has only ~10% the activity of $Mn(III)_2$-Y•-NrdF isolated in eNrdF (Table 1, 27 vs 363 nmol min^{-1} mg^{-1}). This result is similar to the observations we recently reported with *Ec* NrdF (7). While both the iron and manganese cofactors of rNrdF are active in nucleotide reduction, the manganese cofactor is much more active and is the one assembled in vivo.

Discussion

The construction of the *Bs* 1B-UP strain resulted in increased amounts of the four proteins encoded by the *Bs nrdI-nrdE-nrdF-ymaB* operon, facilitating purification of active eNrdF (30). Abs raised to each of the independently expressed recombinant proteins revealed that the levels of NrdE and NrdF in 1B-UP were elevated 35-fold relative to the wt strain. The 18-fold increase of RNR activity in crude cell extracts of 1B-UP relative to the wt strain, demonstrated that NrdF has an active cofactor assembled. The visible and EPR spectra of the purified RNR (Figures 3 and 4) demonstrate the presence of the $Mn(III)_2$-Y• cofactor, similar to that recently characterized in *Ec* and *Ca* (4, 7, 8, 12). In each of these cases, however, manganese was added to the growth media to obtain loaded-NrdF in sufficient quantities for biophysical characterization of the metal center (4, 7, 8, 12), while in the *Bs* case, no Mn(II) addition was required. The Y• content (0.44 Y•/β_2) was also higher than that purified from *Ca* (0.36 Y•/β_2) and *Ec* (0.2 Y•/β_2) (4, 7, 8, 12). Thus, the $Mn(III)_2$-Y• center is also the active cofactor of RNR in *Bs*.

Several surprising observations resulted from the eNrdF purification from the 1B-UP strain. One was that isolation of NrdF was accompanied by NrdE at each step during the purification. This result is consistent with an early report, that fractionation of *Bs* crude cell extracts by size exclusion chromatography gave RNR activity eluting as a large complex (29). However, contradictory studies on the quaternary structure of the *Ca* RNR (12, 31) and our own recent studies using recombinant *Bs* proteins (data not shown) indicate that quaternary structure(s) of active class Ib RNRs require further investigation. We proposed that the quaternary structure and inability to correctly assemble active NrdEF from rNrdF and rNrdE is, in part, responsible for the differences in activities observed between rNrdF and eNrdF.

Our recent studies showed that *Ec* NrdF interacts tightly with *Ec* NrdI, an observation that facilitated its purification from endogenous levels in an engineered *Ec* strain (8). Thus, the second interesting aspect of the purification of *e*NrdF was that, in contrast to the *Ec* results, *Bs* $(His)_6$-NrdI was unable to enrich NrdF from the 1B-UP strain cell lysate by Ni-NTA affinity chromatography. While it is possible that the co-purification of eNrdEF could disrupt its interaction with NrdI, our recent structural studies of the *Ec* NrdINrdF complex suggest that NrdE can be docked onto this complex with no steric interference, using the class Ia RNR docking model ($\alpha_2\beta_2$) (38). Differences in interactions between NrdI and NrdF might have been anticipated from sequence alignments of NrdIs. All NrdIs have a loop that covers the FMN cofactor (designated the 50S loop). In *Bacillus* this loop contains only 3 amino acids, distinct from the two additional subclasses of NrdIs, in which the loop is glycine rich and much longer (18, 26, 27, 38). A recent publication describing the structure of *Ba* NrdI, supports this distinction, as a K_d for its interaction with *Ba* NrdF was reported to be weak (50 μM) (26). These studies suggest that the affinity between the *Bs* NrdI and NrdF is distinct from these interactions in *Ec*.

Additional distinctions between NrdIs from different sources is based on titration studies with dithionite to maximize FMN_{sq}. Results with *Bs* NrdI (32%) are similar to those reported for *Ec* NrdI (30%), but different from *Ba* (60%) and *Bc* (100%) NrdI (18). Our biochemical and structural studies with the complex of *Ec* NrdI•Mn-NrdF (7, 38) suggested

that HOO(H) is the oxidant of manganese. Whether the increased amounts of FMN_{sq} observed in the *Bc* and *Ba* NrdI titrations is indicative of an alternative Mn(II) oxidant, that is $O_2^{\bullet-}$, remains to be established (2).

Further insight into the role of *Bs* NrdI in $Mn(III)_2$-Y• cluster assembly is provided by western analyses of crude cell extracts of wt and 1B-UP strains. NrdI is present at a much lower level relative to NrdEF, and thus likely acts catalytically. We have recently reported a similar observation for the *Ec* class Ib RNR (8). In neither case has the reductase that re-reduces $NrdI_{ox}$ (or $NrdI_{sq}$) been identified. Thus, the substoichiometric $Mn(III)_2$-Y• cluster assembly observed, might be associated with insufficient reductase to recycle NrdI.

Finally, the *Bs* class Ib RNR activity assay requires further investigation. The activity of *Bs* NrdEF and observation that addition of additional rNrdE increases the activity is likely associated with the absence of DTT during the purification of eNrdF and the use of the non-physiological reductant in the assay. While, glutaredoxin or the glutaredoxin-like protein NrdH has been proposed to be the physiological reductant for NrdE in *Ca*, *Ll*, *St*, *Sa*, and *Ec* (33, 36, 37, 39, 40), the absence of NrdH in the *Bs* class Ib operon/genome require an alternative candidate. In *Bs*, the *yosR* gene, encodes a glutaredoxin-like protein and is located near the RNR operon of a prophage origin (SPbeta *bsnrdEF*) (30). While we cannot rule out the possibility that YosR is the endogenous NrdE reductant, we disfavor this proposal as this operon is present only in the genomes of some *Bs* subspecies and *yosR* is nonessential (41, 42). By process of elimination, we consider thioredoxin and thioredoxin reductase as the best candidates for the NrdE reductant, as both genes (*trxA* and *trxB*) are essential (43). The recent discovery of a small thiol molecule, bacillithiol (44), in some gram positive bacteria including *Bs*, suggest that this molecule may also be a candidate for NrdE reduction. Ongoing experiments will answer this question.

In summary, regardless of the source of the $Mn(III)_2$-Y•, reconstituted or endogenous, this cofactor is 13 times more active than the $Fe(III)_2$-Y• rNrdF when assayed under the same conditions. Moreover, the isolation of $Mn(III)_2$-Y•-eNrdF from *Bs* cultured in LB medium without manipulation of the metal content, suggests that *Bs* NrdF is an obligate manganese enzyme. The fact that the $Fe(III)_2$-Y•-rNrdF is also enzymatically active establishes that cells have developed mechanisms to either enhance correct metal insertion or prevent mis-metallation. Such mechanisms could have significant medical implications as these studies further suggest that many pathogenic organisms require a $Mn(III)_2$-Y• cluster to produce deoxynucleotides and probably to escape host defense strategies of limiting iron for the pathogens (13).

Supplementary Material

Refer to Web version on PubMed Central for supplementary material.

Acknowledgments

We thank J. A. Cotruvo, Jr. for developing experimental methods associated with NrdI purification, Mn analysis and determination of the amount of $NrdI_{sq}$. We are grateful to S. J. Lippard (MIT) for use of the atomic absorption spectrometer. We thank C. Lee and A. Grossman (MIT) for the generous gifts of the *Bs* wt JH642 strain, the *Bs* wt JH642 genomic DNA, and their very helpful discussions.

References

1. Nordlund P, Reichard P. Ribonucleotide reductases. Annu Rev Biochem. 2006; 75:681–706. [PubMed: 16756507]

2. Cotruvo JA Jr, Stubbe J. Class I ribonucleotide reductases: Metallocofactor assembly and repair in vitro and in vivo. Annu Rev Biochem. 2011 in press.
3. Stubbe J, Cotruvo JA Jr. Control of metallation and active cofactor assembly in the class Ia and Ib ribonucleotide reductases: diiron or dimanganese? Curr Opin Chem Biol. 2011; 145:284–290. [PubMed: 21216656]
4. Cox N, Ogata H, Stolle P, Reijerse E, Auling G, Lubitz W. A tyrosyl-dimanganese coupled spin system is the native metalloradical cofactor of the R2F subunit of the ribonucleotide reductase of *Corynebacterium ammoniagenes*. J Am Chem Soc. 2010; 132:11197–11213. [PubMed: 20698687]
5. Högbom M, Galander M, Andersson M, Kolberg M, Hofbauer W, Lassmann G, Nordlund P, Lendzian F. Displacement of the tyrosyl radical cofactor in ribonucleotide reductase obtained by single-crystal high-field EPR and 1.4-angstrom x-ray data. Proc Natl Acad Sci U S A. 2003; 100:3209–3214. [PubMed: 12624184]
6. Roca I, Torrents E, Sahlin M, Gibert I, Sjöberg BM. NrdI essentiality for class Ib ribonucleotide reduction in *Streptococcus pyogenes*. J Bacteriol. 2008; 190:4849–4858. [PubMed: 18502861]
7. Cotruvo JA Jr, Stubbe J. An active dimanganese(III)-tyrosyl radical cofactor in *Escherichia coli* class Ib ribonucleotide reductase. Biochemistry. 2010; 49:1297–1309. [PubMed: 20070127]
8. Cotruvo JA, Stubbe J. *Escherichia coli* Class Ib Ribonucleotide Reductase Contains a Dimanganese(III)-Tyrosyl Radical Cofactor in Vivo. Biochemistry. 2011; 50:1672–1681. [PubMed: 21250660]
9. Atkin CL, Thelander L, Reichard P, Lang G. Iron and free-radical in ribonucleotide reductase - exchange of iron and Mössbauer-spectroscopy of protein-B2 subunit of *Escherichia coli* enzyme. J Biol Chem. 1973; 248:7464–7472. [PubMed: 4355582]
10. Ehrenberg A, Reichard P. Electron spin resonance of the iron-containing protein B2 from ribonucleotide reductase. J Biol Chem. 1972; 247:3485–3488. [PubMed: 4337857]
11. Huque Y, Fieschi F, Torrents E, Gibert I, Eliasson R, Reichard P, Sahlin M, Sjöberg BM. The active form of the R2F protein of class Ib ribonucleotide reductase from *Corynebacterium ammoniagenes* is a diferric protein. J Biol Chem. 2000; 275:25365–25371. [PubMed: 10801858]
12. Stolle P, Barckhausen O, Oehlmann W, Knobbe N, Vogt C, Pierik AJ, Schmidt PP, Reijerse EJ, Lubitz W, Auling G. Homologous expression of the *nrdF* gene of *Corynebacterium ammoniagenes* strain ATCC 6872 generates a manganese-metallocofactor (R2F) and a stable tyrosyl radical (Y•) involved in ribonucleotide reduction. FEBS Lett. 2010; 277:4849–4862.
13. Lundin D, Torrents E, Poole AM, Sjöberg BM. RNRdb, a curated database of the universal enzyme family ribonucleotide reductase, reveals a high level of misannotation in sequences deposited to Genbank. BMC Genomics. 2009; 10:589–596. [PubMed: 19995434]
14. Britton RA, Eichenberger P, Gonzalez-Pastor JE, Fawcett P, Monson R, Losick R, Grossman AD. Genome-wide analysis of the stationary-phase sigma factor (sigma-H) regulon of Bacillus subtilis. J Bacteriol. 2002; 184:4881–4890. [PubMed: 12169614]
15. Fish WW. Rapid colorimetric micromethod for the quantitation of complexed iron in biological samples. Methods Enzymol. 1988; 158:357–364. [PubMed: 3374387]
16. Gasteiger, E.; Hoogland, C.; Gattiker, A.; Duvaud, S.; Wilkins, MR.; Appel, RD.; Bairoch, A. Protein identification and analysis tools on the ExPASy server. In: Walker, JM., editor. The Proteomics Protocols Handbook. Humana Press; Totowa, NJ: 2005. p. 571-607.
17. Edmondson DE, Tollin G. Chemical and physical characterization of the Shethna flavoprotein and apoprotein and kinetics and thermodynamics of flavin analog binding to the apoprotein. Biochemistry. 1971; 10:124–132. [PubMed: 5538602]
18. Cotruvo JA Jr, Stubbe J. NrdI, a flavodoxin involved in maintenance of the diferric-tyrosyl radical cofactor in Escherichia coli class Ib ribonucleotide reductase. Proc Natl Acad Sci U S A. 2008; 105:14383–14388. [PubMed: 18799738]
19. Perego M, Spiegelman GB, Hoch JA. Structure of the gene for the transition state regulator, abrB: regulator synthesis is controlled by the spo0A sporulation gene in Bacillus subtilis. Mol Microbiol. 1988; 2:689–699. [PubMed: 3145384]
20. Cutting, SM.; Vander-Horn, PB. Genetic Analysis. In: Harwood, CR.; Cutting, SM., editors. Molecular Biological Methods for Bacillus. John Wiley & Sons, Ltd.; Chichester, England: 1990. p. 27-74.

21. Steeper JR, Steuart CD. A rapid assay for CDP reductase activity in mammalian cell extracts. Anal Biochem. 1970; 34:123–130. [PubMed: 5440901]
22. Malmström BG, Reinhammar B, Vanngard T. The state of copper in stellacyanin and laccase from the lacquer tree Rhus vernicifera. Biochim Biophys Acta. 1970; 205:48–57. [PubMed: 4314765]
23. Laemmli UK. Cleavage of structural proteins during the assembly of the head of bacteriophage T4. Nature. 1970; 227:680–685. [PubMed: 5432063]
24. Torrents E, Sahlin M, Biglino D, Gräslund A, Sjöberg BM. Efficient growth inhibition of *Bacillus anthracis* by knocking out the ribonucleotide reductase tyrosyl radical. Proc Natl Acad Sci USA. 2005; 102:17946–17951. [PubMed: 16322104]
25. Yang F, Curran SC, Li LS, Avarbock D, Graf JD, Chua MM, Lu G, Salem J, Rubin H. Characterization of two genes encoding the *Mycobacterium tuberculosis* ribonucleotide reductase small subunit. J Bacteriol. 1997; 179:6408–6415. [PubMed: 9335290]
26. Johansson R, Torrents E, Lundin D, Sprenger J, Sahlin M, Sjöberg BM, Logan DT. High-resolution crystal structures of the flavoprotein NrdI in oxidized and reduced states -an unusual flavodoxin. FEBS J. 2010; 277:4265–4277. [PubMed: 20831589]
27. Røhr ÅK, Hersleth HP, Andersson KK. Tracking flavin conformations in protein crystal structures with Raman spectroscopy and QM/MM calculations. Angew Chem Int Ed. 2010; 49:2324–2327.
28. Parkin SE, Chen S, Ley BA, Mangravite L, Edmondson DE, Huynh BH, Bollinger JM Jr. Electron injection through a specific pathway determines the outcome of oxygen activation at the diiron cluster in the F208Y mutant of *Escherichia coli* ribonucleotide reductase protein R2. Biochemistry. 1998; 37:1124–1130. [PubMed: 9454605]
29. Mohamed SF, Gvozdiak OR, Stallmann D, Griepenburg U, Follmann H, Auling G. Ribonucleotide reductase in *Bacillus subtilis* - evidence for a Mn-dependent enzyme. BioFactors. 1998; 7:337–344. [PubMed: 9666321]
30. Härtig E, Hartmann A, Schätzle M, Albertini AM, Jahn D. The *Bacillus subtilis nrdEF* genes, encoding a class Ib ribonucleotide reductase, are essential for aerobic and anaerobic growth. Appl Environ Microbiol. 2006; 72:5260–5265. [PubMed: 16885274]
31. Willing A, Follmann H, Auling G. Ribonucleotide reductase of *Brevibacterium ammoniagenes* is a manganese enzyme. Eur J Biochem. 1988; 170:603–611. [PubMed: 2828045]
32. Climent I, Sjoberg BM, Huang CY. Site-directed mutagenesis and deletion of the carboxyl terminus of Escherichia coli ribonucleotide reductase protein R2. Effects on catalytic activity and subunit interaction. Biochemistry. 1992; 31:4801–4807. [PubMed: 1591241]
33. Jordan A, Pontis E, Aslund F, Hellman U, Gibert I, Reichard P. The ribonucleotide reductase system of *Lactococcus lactis* Characterization of an NrdEF enzyme and a new electron transport protein. J Biol Chem. 1996; 271:8779–8785. [PubMed: 8621514]
34. Fontecave M, Gerez C, Mansuy D, Reichard P. Reduction of the Fe(III)-tyrosyl radical center of *Escherichia coli* ribonucleotide reductase by dithiothreitol. J Biol Chem. 1990; 265:10919–10924. [PubMed: 2113527]
35. Mao SS, Yu GX, Chalfoun D, Stubbe J. Characterization of C439SR1, a mutant of Escherichia coli ribonucleotide diphosphate reductase: evidence that C439 is a residue essential for nucleotide reduction and C439SR1 is a protein possessing novel thioredoxin-like activity. Biochemistry. 1992; 31:9752–9759. [PubMed: 1390751]
36. Jordan A, Pontis E, Atta M, Krook M, Gibert I, Barbé J, Reichard P. A second class I ribonucleotide reductase in *Enterobacteriaceae*: Characterization of the *Salmonella typhimurium* enzyme. Proc Natl Acad Sci USA. 1994; 91:12892–12896. [PubMed: 7809142]
37. Rabinovitch I, Yanku M, Yeheskel A, Cohen G, Borovok I, Aharonowitz Y. *Staphylococcus aureus* NrdH-redoxin is a reductant of the class Ib ribonucleotide reductase. J Bacteriol. 2010; 192:4963–4972. [PubMed: 20675493]
38. Boal AK, Cotruvo JA Jr, Stubbe J, Rosenzweig AC. Structural basis for activation of class Ib ribonucleotide reductase. Science. 2010; 329:1526–1530. [PubMed: 20688982]
39. Fieschi F, Torrents E, Toulokhonova L, Jordan A, Hellman U, Barbé J, Gibert I, Karlsson M, Sjöberg BM. The manganese-containing ribonucleotide reductase of *Corynebacterium ammoniagenes* is a class Ib enzyme. J Biol Chem. 1998; 273:4329–4337. [PubMed: 9468481]

40. Jordan A, Aslund F, Pontis E, Reichard P, Holmgren A. Characterization of *Escherichia coli* NrdH. A glutaredoxin-like protein with a thioredoxin-like activity profile. J Biol Chem. 1997; 272:18044–18050. [PubMed: 9218434]

41. Stankovic S, Soldo B, Beric-Bjedov T, Knezevic-Vukcevic J, Simic D, Lazarevic V. Subspecies-specific distribution of intervening sequences in the Bacillus subtilis prophage ribonucleotide reductase genes. Syst Appl Microbiol. 2007; 30:8–15. [PubMed: 16621400]

42. Kobayashi K, Ehrlich SD, Albertini A, Amati G, Andersen KK, Arnaud M, Asai K, Ashikaga S, Aymerich S, Bessieres P, et al. Essential Bacillus subtilis genes. Proc Natl Acad Sci USA. 2003; 100:4678–4683. [PubMed: 12682299]

43. Scharf C, Riethdorf S, Ernst H, Engelmann S, Volker U, Hecker M. Thioredoxin is an essential protein induced by multiple stresses in Bacillus subtilis. J Bacteriol. 1998; 180:1869–1877. [PubMed: 9537387]

44. Newton GL, Rawat M, La Clair JJ, Jothivasan VK, Budiarto T, Hamilton CJ, Claiborne A, Helmann JD, Fahey RC. Bacillithiol is an antioxidant thiol produced in Bacilli. Nat Chem Biol. 2009; 5:625–627. [PubMed: 19578333]

45. Högbom M, Stenmark P, Voevodskaya N, McClarty G, Gräslund A, Nordlund P. The radical site in chlamydial ribonucleotide reductase defines a new R2 subclass. Science. 2004; 305:245–248. [PubMed: 15247479]

46. Jiang W, Yun D, Saleh L, Barr EW, Xing G, Hoffart LM, Maslak MA, Krebs C, Bollinger JMJ. A manganese(IV)/iron(III) cofactor in *Chlamydia trachomatis* ribonucleotide reductase. Science. 2007; 316:1188–1191. [PubMed: 17525338]

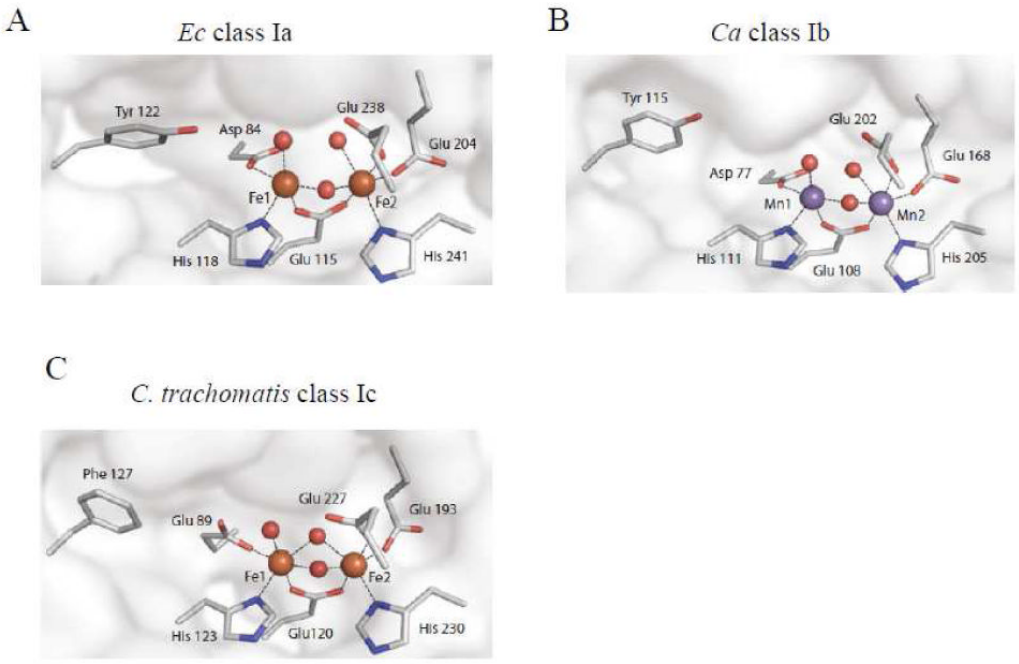

Figure 1.

Structures of the metallocofactors of the three class I RNRs (adapted from (2)). Iron and manganese ions are depicted as brown and purple spheres, respectively. A. *Ec* class Ia $Fe(III)_2$ cluster (5); B. *Ca* Ib $Mn(III)_2$ cluster (4); C. *C. trachomatis* class Ic $Fe(III)_2$ cluster (45). Note that *C. trachomatis* class Ic RNR is active with a $Mn^{IV}Fe^{III}$ cofactor (46) but a structure is not yet available.

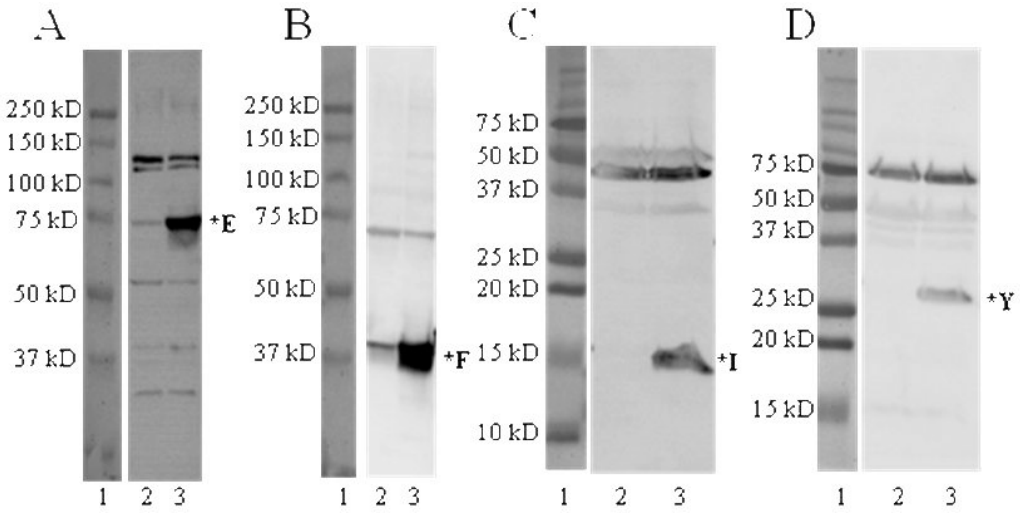

Figure 2.
Western blots of NrdE (A), NrdF (B), NrdI (C) and YmaB (D) in wt and 1B-UP *Bs* strains. Lane 1, molecular weight standards; Lane 2, wt strain; Lane 3, 1B-UP strain.

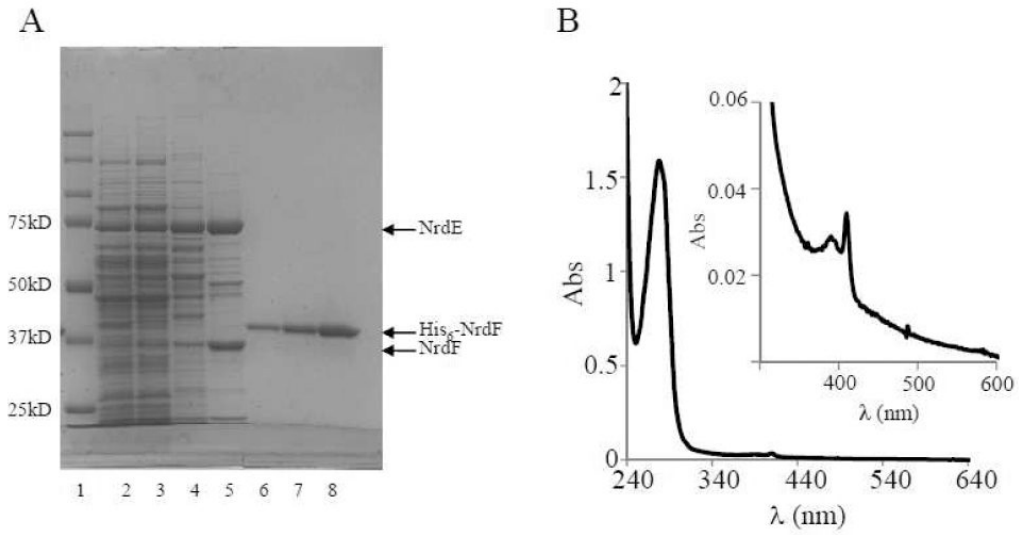

Figure 3.

Purification of the eNrdF from the *Bs* 1B-UP strain. A. Samples from each step of the purification were loaded on a 10% SDS-PAGE gel. Lane 1, protein molecular weight markers; Lane 2, 30 μg of crude cell extracts; Lane 3, 30 μg after ammonium sulfate precipitation; Lane 4, 15 μg after Butyl Sepharose chromatography; Lane 5, 10 μg after FPLC Poros HQ20; Lane 6-8, $(His)_6$-rNrdF loaded at 1, 2, 4 μg. B. Vis spectrum of eNrdF. Inset, enlargement to magnify the features of the $Mn(III)_2$-Y• cluster.

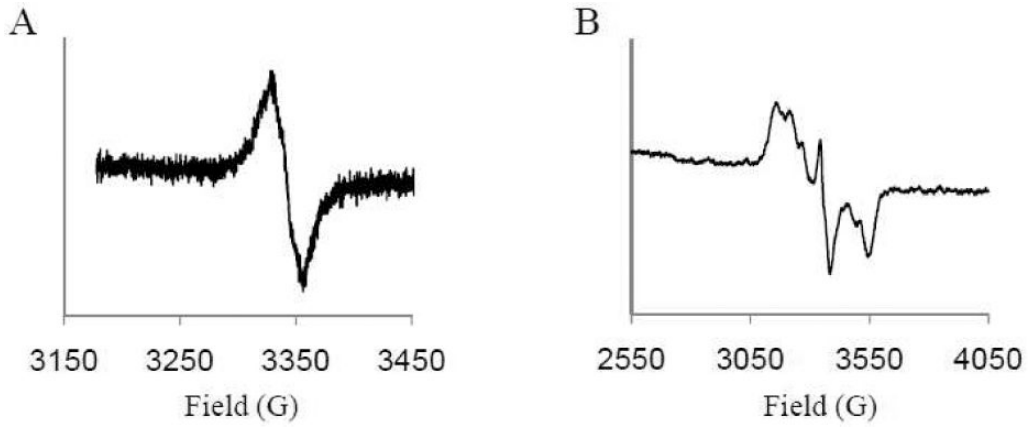

Figure 4.

X-band EPR spectra of the eNrdF at 77 (A) and 4 K (B). A. The spectrum was taken at 77 K at 9.4 GHz, 1 mW power, 2.52×10^4 gain, 1.5 G modulation amplitude, and 100 kHz modulation frequency. B. The spectrum was taken at 4 K, 9.4 GHz, 1 mW power, 1.26×10^4 gain, 4.0 G modulation amplitude, and 100 kHz modulation frequency.

Table 1
SA of $Fe(III)_2$-Y• -rNrdF and $Mn(III)_2$-Y• eNrdF

	$Fe(III)_2$-Y• rNrdF (0.8Y•)[a]		$Mn(III)_2$-Y• eNrdF (0.4Y•)[b]	
	ATP	**dATP**	**ATP**	**dATP**
SA[c]	22	15	160	52
SA[c] per Y•	27	19	363	117

[a] Purified from *Ec* and reconstituted by addition of Fe(II) to crude extracts;

[b] Purified from *Bs*;

[c] SA was measured with ATP or dATP as allosteric effector and is given in nmol min^{-1} mg^{-1}.

Biochemistry. Author manuscript; available in PMC 2012 June 28.

Table 2

Purification of eNrdF from *Bs* 1B-UP strain[a]

Step[b]	Vol (mL)	Conc. (mg/mL)	Protein (mg)	SA[c] (U/mg)	TA[d] (U)	Yield (%)
Lysate	10	15.2	152	0.85	129	100
AS	10.7	7	74.5	0.65	48.1	37.3
Butyl	1	7.5	7.5	1.94	14.5	11.2
FPLC	0.42	1.1	0.5	17.2[e]	8.1	6.3

[a] Purified from 2.9 g cell paste;

[b] Lysate, AS, Butyl, FPLC represent crude cell lysate, ammonium sulfate precipitate, protein after Butyl Sepharose and FPLC Poros HQ20 chromatographies, respectively;

[c] SAs were measured using dATP as allosteric effector and are given as nmol min^{-1} mg^{-1} total protein;

[d] Total activity;

[e] Purified eNrdF. The SA for NrdF of eNrdF is therefore 52 nmol min^{-1} mg^{-1} and 117 nmol min^{-1} mg^{-1} (normalized for 1 Y•) (Table 1).

Table 3

Metal content of rNrdF and eNrdF

	$Fe(III)_2$-Y• rNrdF[a]	**$Mn(III)_2$-Y• NrdF[b]**
Y•/β_2	0.18	0.44
Mn/β_2	0.038	1.8-2.4
Fe/β_2	0.9	0.14

[a] Purified from *Ec*;

[b] purified from *Bs*.